Journal Pre-proof

Improvement in oxidative stability of versatile peroxidase by flow cytometry-based high-throughput screening system

Karla Ilić Đurđić (Conceptualization) (Investigation) (Writing - original draft), Selin Ece (Methodology) (Investigation), Raluca Ostafe (Methodology) (Validation), Simon Vogel (Validation) (Visualization), Stefan Schillberg (Writing - review and editing) (Resources), Rainer Fischer (Writing - review and editing) (Resources), Radivoje Prodanović (Conceptualization) (Supervision) (Project administration) (Writing - review and editing)

PII: S1369-703X(20)30070-X

DOI: https://doi.org/10.1016/j.bej.2020.107555

Reference: BEJ 107555

To appear in: *Biochemical Engineering Journal*

Received Date: 6 October 2019

Revised Date: 6 March 2020

Accepted Date: 8 March 2020

Please cite this article as: Đurđić KI, Ece S, Ostafe R, Vogel S, Schillberg S, Fischer R, Prodanović R, Improvement in oxidative stability of versatile peroxidase by flow cytometry-based high-throughput screening system, *Biochemical Engineering Journal* (2020), doi: https://doi.org/10.1016/j.bej.2020.107555

Biochemical Engineering Journal

Research article

Improvement in oxidative stability of versatile peroxidase by flow cytometry-based high-throughput screening system

Karla Ilić Đurđić[1], Selin Ece[2,3], Raluca Ostafe[3,4], Simon Vogel[5], Stefan Schillberg[5], Rainer Fischer [3,6], Radivoje Prodanović[1]

[1]University of Belgrade-Faculty of Chemistry, Studentski trg 12-16, 11000 Belgrade, Serbia

[2] PerkinElmer chemagen Technologie GmbH, Arnold-Sommerfeld-Ring 2, 52499 Baesweiler, Germany

[3] Institute of Molecular Biotechnology, RWTH Aachen University Worringerweg 1, 52074 Aachen, Germany

[4] Purdue Institute of Inflammation, Immunology and Infectious Disease; Molecular Evolution, Protein Engineering and Production; Purdue University, 207 S. Martin Jischke Dr., West Lafayette, IN 47907, USA

[5] Fraunhofer Institute for Molecular Biology and Applied Ecology IME, Forckenbeckstrasse 6, 52074 Aachen, Germany

[6] Departments of Biological Sciences and Chemistry, Purdue University, 207 S. Martin Jischke Dr., West Lafayette, IN 47907, USA

Correspondence: Prof. Radivoje Prodanović, University of Belgrade-Faculty of Chemistry, Studentski trg 12-16, 11000 Belgrade, Serbia.

E-mail: rprodano@chem.bg.ac.rs

Graphical abstract

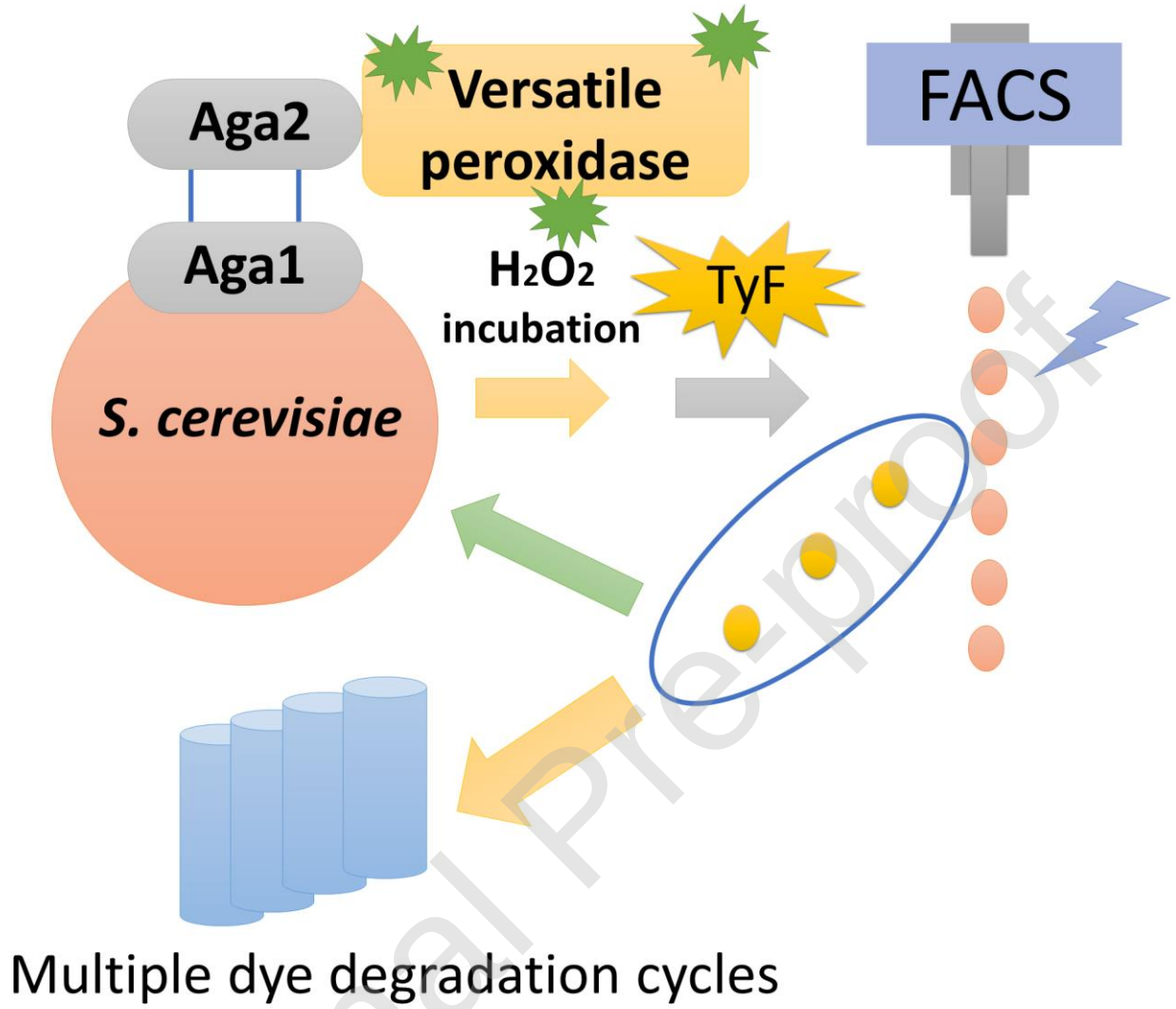

Highlights

- Versatile peroxidase library was generated using error prone PCR.
- Variants were expressed on yeast cell surface and screened using FACS-based method.
- Mutants retaining activity after 1h peroxide incubation were selected.
- Mutants with 1.5 times increased catalytic constant were found.
- Azo dyes were decolorized using mutant enzymes immobilized within cell wall.

Abstract

Pleurotus eryngii wild-type versatile peroxidase (wtVP) oxidizes structurally diverse substrates in an H_2O_2-dependent manner, but its ability to oxidize many pollutants is limited by suicidal enzyme inactivation in the presence of excess H_2O_2. To address this drawback, we generated random mutagenesis libraries containing 3×10^6 mutated VP genes and screened for enzymes with higher oxidative stability expressed on the surface of yeast cells. This was achieved by flow cytometry using the substrate fluorescein tyramide. After two rounds of sorting, the percentage of cells expressing variants with improved oxidative stability had increased from 1% to 56%. The most stable variants featured 3–5 amino acid substitutions and retained up to 70% of their initial activity after incubation for 1 h in 30 mM H_2O_2 (conditions that completely inactivate wtVP). Selected variants were extracted from yeast cell walls and purified for kinetic characterization. We also prepared yeast cell walls with wtVP and the three most stable VP variants for multiple cycles of azo dye (Reactive black 5) degradation. After 10 cycles of 12 h, two of the variants retained more than 97% of their initial activity, whereas the activity of wtVP declined by ~30%. These results confirm that our high-throughput screening system can improve the oxidative stability of versatile peroxidase, providing a source of novel enzymes for remediation applications.

Keywords

Directed evolution, FACS, hydrogen-peroxide stability, yeast surface display

1. Introduction

Versatile peroxidase (VP) is a class II heme-containing oxidoreductase secreted by certain fungi as a part of the lignin-degradation consortium [1,2]. VP is produced by many basidiomycetes, including the genera *Pleurotus* [3,4]. VP combines the catalytic cycles of two other ligninolytic

peroxidases: lignin peroxidase (LiP) and manganese peroxidase (MnP) [5,6]. The H_2O_2-mediated oxidation of compounds with a high redox potential involves a long-range electron transfer (LRET) pathway from the heme group in the enzyme's central cavity to the Trp164 residue on the surface [7,8]. VP also oxidizes Mn^{2+} due to the presence of an oxidation site with a channel extending directly to the heme molecule. Mn^{3+} acts as diffusible oxidant for a wide range of phenolic and non-phenolic substrates [9]. A third oxidation site connected to the main heme access channel is responsible for the oxidation of compounds with a lower redox potential [5].

The presence of multiple oxidation sites for substrates with different redox potentials enables the oxidation of a wide range of substrates, making VP suitable for many industrial and environmental applications [10]. In addition to delignification [11] and the synthesis of new compounds [12,13], VPs are ideal for the degradation of phenolic and non-phenolic pollutants, pesticides, pharmaceuticals and industrial dyes [14-19] without additional redox mediators [20-23]. However, the applications of VPs are limited by the suicidal inactivation of the enzyme in the presence of excess of H_2O_2, a substrate required for all oxidation reactions. High levels of H_2O_2 accelerate the formation of superoxide anion radicals containing Fe^{3+}, which are catalytically inactive reaction intermediates. These can trigger the oxidation of amino acids or heme groups, leading to irreversible enzyme inactivation [24-26].

Directed evolution is a powerful tool for the improvement of industrially relevant enzymes, but requires the construction and screening of random mutagenesis gene libraries to identify the best-performing variants [27, 28]. Ideally, it should be possible to select improved variants from a large starting population (up to 10^7 clones) and the screening process should preserve the linkage between genotype and phenotype in order to trace back selected protein characteristics to the corresponding mutations [29]. Linkage can be achieved by the transformation of bacteria or

yeasts with a gene pool library followed by the recovery of single-cell library colonies on solid media or in individual microtiter plate wells. However, this approach is limited to 10^3–10^4 variants per screening round, and the inclusion of such as small number of mutants can lead to the omission of the most active or stable variants in the library [30]. In contrast, cell sorting based on enzyme activity can be achieved by flow cytometry/fluorescence activated cell sorting (FACS), and this allows the screening of more than 10^7 variants per hour [31].

Expression of VP in *E. coli* (most-widely applied host for directed evolution) results in improper folding and high yield of inclusion bodies. Enzyme refolding can be attempted, however, that strategy is not appropriate for high-throughput screening studies [32]. Functional expression of VP in *S. cerevisiae* has been reported [32], along with functional expression of LiP on *S. cerevisiae* cell surface [33]. The major benefit of protein expression on *S. cerevisiae* cell surface is preservation of the link between genotype and phenotype [34-36]. In the most widely-used system, recombinant proteins are fused to the C-terminus of the α-agglutinin mating protein Aga2 [37,38]. Following the galactose-inducible expression of Aga2 fusion proteins, the Aga2 domain forms two disulfide bonds with the Aga1 domain of α-agglutinin anchored in the yeast cell wall, such that the recombinant protein of interest is displayed on the cell surface.

Here we describe the preparation of a mutagenesis library starting with the wild-type VP (wtVP) from the oyster mushroom *Pleurotus eryngii*. The wtVP and mutated variants were expressed as Aga2 fusion proteins and displayed on the surface of yeast cells, allowing the application of flow cytometry for high-throughput library screening in order to select VP variants with increased stability in the presence of H_2O_2.

2. Materials and methods

2.1 Chemical synthesis

Fluorescein tyramide (TyrF) was used as a substrate for VP activity screening, and was synthesized as previously described [39] with minor adjustments. We mixed 20 mM tyramine HCl with 25 mM triethylamine and 20 mM *N*-hydroxysuccinimide-fluorescein (all dissolved in dimethyl formamide) and incubated the mixture at 4 °C for 3 h. The product was diluted in ethanol to a final concentration of 2 mM and was stored in dark at 4 °C.

2.2 Preparation of the *P. eryngii* VT sequence and transfer to vector pCTCON2

The *P. eryngii* gene encoding wtVP (**Fig. S1**) was synthesized by Eurofins Genomics (Ebersberg, Germany) and transferred to the yeast surface display vector pCTCON2 (kindly provided by Professor Dane Wittrup, Massachusetts Institute of Technology) at the NheI and BamHI sites (**Fig. S2**) to generate recombinant construct wtVP-pCTCON2 (**Fig. S3**). After ligation, the mixture was used for the transformation of *Escherichia coli* XL10Gold cells (Agilent Technologies, Santa Clara, CA, USA) according to the manufacturer's instructions. The integrity of wtVP-pCTCON2 was confirmed by sequencing using the primers listed in **Table S1**, and plasmid DNA was isolated using the NucleoSpin plasmid isolation kit (Macherey-Nagel, Düren, Germany) according to the manufacturer's instructions.

2.3 Preparation of random mutagenesis libraries

Random mutagenesis gene libraries were prepared using the Gene Morph II random mutagenesis kit (Agilent Technologies) with VP-pCTCON2 as the template. Two gene libraries with two different mutation rates were prepared using two different concentrations of target DNA and the primer sequences listed in **Table S1**. The PCR mixtures comprised 300 or 50 pg/µL of target DNA, 100 nM of primers and the remaining kit components. Each reaction began with a 95 °C denaturation step for 2 min, followed by 35 cycles of 95 °C for 30 s, 60 °C for 30 s and 72 °C for 1 min, and a final extension step at 72 °C for 10 min. The template DNA was digested with DpnI

for 90 min at 37 °C, and the products were purified using the PCR purification and gel extraction kit (Macherey-Nagel).

The mutated genes were used as megaprimers for the amplification of whole plasmid DNA [40]. The PCR mixtures contained 5 ng/µL megaprimers and 6 ng/µL template DNA (VP-pCTCON2), 3% (v/v) DMSO, and Q5 Hot Start High-Fidelity 2× Master Mix (New England BioLabs, Ipswich, MA, USA). Each reaction started with a 95 °C denaturation step for 30 s, followed by 35 cycles of 95 °C for 10 s, 61 °C for 30 s and 72 °C for 5 min, and a final extension step at 72 °C for 10 min. The template was digested with DpnI and the products were used directly for the transformation of *E. coli* XL10Gold ultra competent cells as above. Plasmid DNA was isolated using the NucleoSpin plasmid isolation kit and the presence of mutations was confirmed by sequencing 10 randomly selected mutants.

2.4 Expression of VP on the yeast cell surface

Plasmids from both libraries were pooled for the transformation of *S. cerevisiae* EBY100 cells (kindly provided by Professor Dane Wittrup, Massachusetts Institute of Technology), and controls were prepared with the pCTCON2 base vector and the wtVP-pCTCON2 construct [41]. Transformation was promoted by exposing the cells to a 42 ºC heat-shock step for 1 h, and transformants were selected on YNB-CAA plates with 2% (w/v) glucose. For the cells transformed with pCTCON2 or wtVP-pCTCON2, single colonies from YNB-CAA plates were inoculated into 20 mL YNB-CAA medium with 2% (w/v) glucose and 50 µg/mL chloramphenicol. The cells transformed with the library plasmid pool were collected and inoculated into 20 mL of the same medium. All liquid cultures were incubated at 28 °C, shaking at 160 rpm, until the optical density at 600 nm (OD_{600}) reached 3–3.5 (approximately 16 h). Enzyme expression was induced by transferring cells from the glucose culture into YNB-CAA

medium with 2% (w/v) galactose and 50 µg/mL chloramphenicol to achieve an initial OD_{600} of 0.8 (final volume of 20 mL) and adding 20 µL 0.5 M 5-aminolevulinic acid (final concentration 500 µM). The cells were cultivated as above for a further 16 h.

2.5 Fluorescein tyramide assay

The TyrF assay was adapted from a previous report [42]. Briefly, the yeast cells from the 16-h incubation described above were washed three times with 100 mM sodium acetate (pH 4.5) at a concentration of 10^8 cells/mL (where $OD_{600} = 1$ refers to 2×10^7 cells/mL) and resuspended in the same buffer containing 0.1% (w/v) bovine serum albumin (BSA). Reactions were carried out in 200-µL aliquots containing 2×10^6 cells, 20 µM TyrF and 1 mM H_2O_2 (TyrF reaction). After 1 min, each reaction was stopped by adding 1 mL 0.5% (w/v) BSA and 10 mM ascorbic acid in 10× PBS. The cells were washed three times with PBS containing 0.1% (w/v) BSA and resuspended in 1 mL of the same buffer. The cells transformed with the empty pCTCON2 or wtVP-pCTCON2 vectors were treated in the same way.

For the sorting of reference libraries, the cells transformed with the empty vector were mixed with those expressing wtVP in different proportions (1%, 5% and 30% of wtVP and 99%, 95% and 70% of pCTCON2, respectively) before the reaction. For oxidative stability tests, 2×10^6 cells were incubated in 30 mM H_2O_2 for 20 min before each sorting round and were washed three times with 100 mM sodium acetate (pH 4.5) containing 0.1% (w/v) BSA and resuspended in 200 µL of the same buffer for the assay. For each sorting round a total of 10^7 cells were analyzed.

2.6 Flow cytometry

Yeast cells were analyzed using a BD FACS Influx flow cytometry system (BD Biosciences, San Jose, CA, USA) with 488-nm laser excitation and a 530-nm emission filter (bandwidth 530/40). The analysis rate was 1000–5000 events/s and the sorting rate was 10–200 events/s. Cells

expressing active VP variants were gated on fluorescence/forward scatter plots specified for every experiment. For reference libraries, three times 400 cells were sorted in a single mode onto YNB-CAA plates containing 2% glucose and 50 µg/mL chloramphenicol. For random mutagenesis libraries, 10^4 cells were sorted onto the same type of plates and liquid medium for multiple sorting rounds, followed by cultivation as described above.

2.7 Microtiter plate assay

Sorted cells were recovered on YNB-CAA plates and single colonies from the plates were inoculated into individual wells of 96-well plates containing 100 µL YNB-CAA medium with 2% (w/v) glucose and 50 µg/mL chloramphenicol. The plates were incubated at 25 °C for 16 h (80% humidity), shaking at 500 rpm. We then transferred 5 µL from each well to a fresh microtiter plate in which each well contained 30 µL of the same medium, and incubated the plates under the conditions described above for a further 8 h. We then added 100 µL YNB-CAA medium with 2% (w/v) galactose, 50 µg/mL chloramphenicol and 500 µM 5-aminolevulinic acid and incubated for a further 16 h to induce VP expression.

The cells were washed three times with 100 mM sodium tartrate buffer (pH 3.5) and 20 µL was transferred from each well to a fresh microtiter plate (MTP) in which each well contained 150 µL of the same buffer. The OD_{600} was determined, and we then added 10 µL 100 mM H_2O_2 and 20 µL 20 mM 2,2'-azino-bis-3-bthylbenzothiazoline 6-sulfonic acid (ABTS) to each well ($\varepsilon_{ABTS\cdot+}$ = 36000 $M^{-1}cm^{-1}$) [37]. For each measurement, we calculated the slope of the linear region normalized to the OD_{600} of the cells in each well. For standardization, three wtVP clones were included in every plate as well as three clones transformed with the empty pCTCON2 vector. For oxidative stability mutants, we pre-incubated the cells with 30 mM H_2O_2 for 30 min. VP activity was measured as described above, and measurements were taken before and after each round of

sorting. All experiments were carried out three times and all measurements were taken in triplicate. For reference mixes total of three MTP were screened for each sorting. For oxidative stability sorting total of 300 cells were analyzed for each sorting round. All measurements were done in triplicates. The mean was calculated considering all measurements, standard deviation was calculated using following equation: $\sigma = \sqrt{\frac{1}{N}\sum_{i=1}^{N}(xi - \mu)^2}$ and standard error was calculated using following equation: $(\sigma_\mu) = \frac{\sigma}{\sqrt{N}}$. For all measurements, the cells expressing the enzyme variant with less than 10% of wtVP activity were marked as not active. For stability measurements, after cell sorting, residual activities after incubation in H_2O_2 were compared with wtVP residual activity. The cells expressing the variants with residual activity whose mean minus two standard deviations were higher than residual activity mean plus two standard deviations for wtVP were marked as more stable than wtVP and the cells expressing the variants whose residual activity mean plus two standard deviations were lower than residual activity mean plus minus standard deviations for wtVP were marked as less stable than wtVP. All other cells were marked as equally stable as wtVP.

2.8 Isolation of selected VP variant plasmids

Plasmids encoding the VP variants with the highest residual activity after exposure to H_2O_2 were isolated as previously described, with modifications [43]. Briefly, three individual clones with the highest residual activity were transferred to 2 mL YNB-CAA medium with 2% (w/v) glucose and 50 µg/mL chloramphenicol and were incubated at 28 ºC for 24 h. The cells were collected and resuspended in 500 µL lysis buffer (50 mM Tris-HCl pH 7.5, 10 mM EDTA, 0.5% (v/v) 2-mercaptoethanol) supplemented with 50 U *Arthrobacter luteus* lyticase and incubated at 30 ºC for 2 h, followed by plasmid isolation as described above. The VP sequences were determined and the plasmids were used for the retransformation of *S. cerevisiae* EBY100 cells.

2.9 Oxidative stability measurements

Retransformed yeast cells expressing VP mutants were washed three times with water, suspended in 3% (v/v) toluene, and lysed at 25 ºC for 6 h, shaking at 200 rpm. After lysis, the cell walls were washed 10 times in reaction buffer (100 mM sodium tartrate, pH 3.5) to remove all traces of toluene. The prepared cell wall fragments were then incubated in 30 mM H_2O_2 for different time periods from 10 min to 1 h. Aliquots taken after 5, 10, 15, 30, 45 and 60 min were diluted to OD_{600} = 1 and VP activity was measured in 100 mM sodium tartrate (pH 3.5) containing 0.5 mM H_2O_2 and 2 mM ABTS. The most stable variants were tested for their ability to degrade the dye Reactive Black 5 in 10 reaction cycles. Cell walls containing wtVP or selected VP variants were mixed with the dye at a concentration of 1 mM and the mixture was supplemented with 0.5 mM H_2O_2. After 12 h, the cell wall fragments were washed and reused for a new degradation cycle with fresh reagents. All experiments were conducted three times and all measurements were done in triplicates. Standard deviations were calculated using following equation: $\sigma = \sqrt{\frac{1}{N}\sum_{i=1}^{N}(xi-\mu)^2}$ considering all measurements and standard error was calculated using following equation: $(\sigma_\mu) = \frac{\sigma}{\sqrt{N}}$.

2.10 Extraction of Aga2-VP fusion proteins from yeast cell walls

The wtVP and selected variants were isolated from 500 mL of culture by centrifugation at 3000×g for 5 min at 4 ºC, followed by resuspending the cell pellet in 50 mL 100 mM sodium acetate (pH 5.5) containing 1 mM 2-mercaptoethanol. The suspension was incubated at 4 ºC for 4 h before repeating the centrifugation step [44]. The supernatant containing Aga2-VP fusion proteins was concentrated using Vivaspin ultrafiltration columns with a molecular weight cutoff of 10 kDa (Sartorius-Stedim, Göttingen, Germany) and the concentrated supernatants were

dialyzed against 20 mM sodium phosphate buffer (pH 7.4). The proteins were purified using Vivapure Q Mini H mini spin columns (Sartorius-Stedim). Fractions containing active Aga2-VP variants were collected and analyzed by denaturing sodium dodecylsulfate polyacrylamide gel electrophoresis (SDS-PAGE) in 12% polyacrylamide gels containing 2-mercaptoethanol. Protein bands were revealed by staining with Coomassie Brilliant Blue R-250 and compared to molecular weight standards (Thermo Fisher Scientific, Waltham, MA, USA). Native electrophoresis was performed under the same running conditions in gels lacking SDS and 2-mercaptoethanol. For zymography, the gel was supplemented with 100 mM sodium tartrate (pH 3.5) containing 0.5 mM H_2O_2 and 9 mM guaiacol [44].

2.11 Characterization of enzyme properties

Kinetic constants for H_2O_2 were estimated by measuring enzyme activity in different concentrations of H_2O_2 (10–800 µM) in 100 mM sodium tartrate buffer (pH 3.5) with 2 mM ABTS as a reducing substrate, taking into account the reaction stoichiometry (two molecules of ABTS are oxidized for each molecule of H_2O_2) as described by Garcia-Ruiz et al. [32]. The concentration of fusion proteins was determined by measuring the absorbance at 280 nm based on an extinction coefficient of 17585 $M^{-1}cm^{-1}$ calculated using ProtParam. All measurements were done in triplicates, standard deviations were calculated using following equation: $\sigma = \sqrt{\frac{1}{N}\sum_{i=1}^{N}(xi-\mu)^2}$ and standard error was calculated using following equation: $(\sigma_\mu) = \frac{\sigma}{\sqrt{N}}$.

3. Results and discussion

The *P. eryngii* wtVP gene was transferred to the expression vector pCTCON2 and used as a template at different concentrations for the preparation of two random mutagenesis libraries with different mutation rates. The clones were expressed as C-terminal fusions to the α-agglutinin

mating protein (Aga2) subunit, which forms two disulfide bonds with the Aga1 domain embedded in the cell wall. Fusion protein expression was induced by switching to galactose supplemented medium, causing VP to be displayed on the surface of the yeast cells. Cells displaying VP libraries were used for flow cytometry-based sorting to select VP variants with increased oxidative stability. Accordingly, the cells were pre-incubated with 30 mM H_2O_2, washed, and exposed to TyrF in the presence of 1 mM H_2O_2 to promote the formation of a TyrF radical that covalently binds to proteins on the cell surface [42]. Following multiple washes to remove excess TyrF, the cells were gated on FITC/forward scatter plots and those with the highest enzymatic activity (brightest green fluorescence) were selected by FACS and recovered on YNB-CAA plates. The best candidates were selected for a second round of sorting after exposing them once again to 30 mM H_2O_2. The VP variants sorted in the second round were tested in microtiter plates to identify those with the highest residual enzymatic activity after H_2O_2 exposure. VP variants showing the highest oxidative stability (residual activity) were sequenced and characterized in more detail. The overview of conducted experiments is presented in **Fig. 1**.

3.1 Reference library sorting

VPs are suitable for many applications, so attempts have been made to improve industrially relevant characteristics such as oxidative, pH and thermal stability [32,45]. Some of these attempts were based on rational design [45] and others on directed evolution [32]. However, current screening systems involve microtiter plate assays that are not appropriate for random mutagenesis libraries with a complexity exceeding 10^4 variants [32,46,47]. To address this issue, we developed the first high-throughput screening system suitable for the isolation of VP variants with enhanced stability in the presence of H_2O_2. A TyrF-based screening system without compartmentalization has previously been used to modify the enantioselectivity of horseradish

peroxidase [44], but such a system has never been used before for ligninolytic peroxidases or in screens for enzyme stability.

Reference libraries were prepared by mixing different ratios of yeast cells expressing wtVPs with cells transformed with the empty pCTCON2 vector (1% of VP-expressing cells and 99% of empty cells – 1% reference mix; 5% of VP-expressing cells and 95% of empty cells – 5% reference mix and 30% of VP-expressing cells and 70% of empty cells – 30% reference mix). Gating was based on differences in fluorescence between 100% empty and 100% positive cells (**Fig. 2**). There was a clear correlation between percentage of active cells added to the mixture and cells with high green fluorescence – indicator of VP activity (**Fig. 2A**). The number of the cells detected in gate number 1 increased from 589 for 1% reference mixture to 2496 for 30% reference mixture (**Fig. 2B**). After sorting, the gated cells were recovered on YNB-CAA plates supplemented with glucose and chloramphenicol. A small population of cells with intense green fluorescence was observed even among the cells transformed with pCTCON2 (the cells in gate number 1), but only ~300 of the 400 sorted cells were recovered on agar plates, probably reflecting the membrane permeability of dead cells allowing the uptake of the fluorescent substrate [46].

VP activity was measured using an ABTS microtiter plate assay. The level of enrichment was dependent on the proportion of positive cells in the reference library (**Fig. 2B**). The percentage of active cells after sorting was highest for the 5% reference library with the final purity close to 70%. The purity of sorted cells was also reported to increase when using TyrF as a substrate for the sorting of glucose oxidase reference libraries, although in that case the sorting process involved single emulsions [47] in contrast to our system lacking compartmentalization. A similar level of enrichment in 5% reference libraries (61%) was also reported during the screening of

cellulase in double emulsions with a different substrate [48]. The sorting of active cells at lower concentrations, such as our 1% reference library, can be affected by background noise and measurement errors [47]. On the other hand, slightly less effective enrichment achieved with the 30% reference library may reflect the cross-reactivity triggered by the larger number of positive cells, resulting in nearby cells that do not express VP also showing a positive signal. Increasing the proportion of cells expressing VP also shifts the entire population toward more intense green fluorescence. This difference should not be significant enough to affect sorting of random mutagenesis libraries. Also, percentage of active cells before sorting was kept lower than 15%.

3.2 Preparation of VP random mutagenesis libraries

Random mutagenesis libraries were prepared by using Mutazyme DNA polymerase to introduce mutations into the wtVP gene followed by whole plasmid amplification with the mutated genes as megaprimers and VP-pCTCON2 as the template. Two libraries with different mutation rates were generated to achieve more diversity among the VP variants. The presence of mutations was verified by sequencing 10 randomly selected mutants from each library. We detected 0–5 mutations per gene in the library with the lower mutation rate (median = 2) and 1–9 mutations in the library with the higher mutation rate (median = 4). Sequencing revealed that the mutations were spread throughout the gene and there were no nucleotide conversion preferences (data not shown). The libraries were pooled to produce a single library with a complexity of 3×10^6, which is similar to or larger than previously reported random mutagenesis libraries used for sorting by flow cytometry [42,44, 49]. Working library size was estimated based on number of single *E. coli* colonies collected from LB-amp-agar plates after transformation and plating of library sample.

3.3 Sorting for oxidative stability

To sort our random mutagenesis libraries for VP mutants with increased oxidative stability, we pre-incubated cells with 30 mM H_2O_2 and took FACS recordings before incubation and 20 min afterwards (**Fig. 3**). Gates were set based on the difference between 100% empty and 100% positive cells as described above. There was no significant difference between the number of events in the gate number 2 for the 100% empty (negative control) cells before and after incubation, but the number of active cells expressing wtVP was much lower after pre-incubation, with 40–50% remaining active. Furthermore, the entire population of the VP library showed significantly lower fluorescence after pre-incubation compared to the same population before. Having optimized the screening procedure, we therefore conducted two rounds of sorting to screen the VP libraries for enzymes with enhanced oxidative stability.

In both sorting rounds, the cells were pre-incubated in 30 mM H_2O_2 for 20 min, and FACS recordings were taken before and after incubation. Increasing peroxide concentrations above 30 mM resulted in a very low cell recovery after sorting of the cells on YNB-CAA plates. There was only a slight increase in the number of active cells detected *before* incubation after two rounds of sorting, but a much more significant increase in the number of active cells detected *after* incubation. Before sorting, only 53% of the cells were active after incubation in 30 mM H_2O_2, but this increased to 72% after the first sorting round (**Fig. 4A**) and to 82% after the second (**Fig. 4B**). Following the recovery of cells on YNB-CAA plates, the clones were transferred to the same medium in microtiter plates and the VP activity was measured using an ABTS microtiter plate assay before and after incubation in 30 mM H_2O_2 for 30 min. We calculated the proportion of cells expressing no active enzyme as well as the proportion expressing VP variants with lower, similar and higher oxidative stability compared to wtVP (**Fig. 4C**). After one round of sorting, the proportion of cells showing no VP activity dropped from 62% to 26%, and after the second round this fell again to 21%, matching the higher number of cells in gate number 3 at the FACS

traces. The enrichment of stable variants was significant during both rounds of sorting: only 1% of the variants showed greater oxidative stability than wtVP prior to sorting, but this increased to 35% after one round and to 56% after two rounds. The proportion of VP variants with similar and lower oxidative stability varied between rounds. The most stable variants were selected for further characterization.

3.4 Characterization of selected VP variants

The oxidative stability of wtVP and selected variants was determined by following residual activity after 10, 20, 30, 40, 50 and 60-minute pre-incubation in 30 mM H_2O_2. Activity was measured with the MTP ABTS assay in 0.5 mM H_2O_2 using VP-coated cell wall fragments after yeast toluene-induced cell lysis (**Fig. S4 and S5**). After pre-incubation in H_2O_2 and before activity measurements the VP-coated yeast cell walls were washed three times with reaction buffer. MV1 retained more than 50% of initial activity after 1 hour of pre-incubation in 30 mM H_2O_2, MV2 more than 60% and MV3 more than 70% of activity, while activity of wtVP could not be detected after more than 50 minutes of pre-incubation (**Fig. 6A**).

Three VP variants (MV1, MV2 and MV3), which showed the highest residual activity after exposure to H_2O_2 based on two rounds of sorting, were selected for further characterization. The corresponding plasmids were prepared in *E. coli* XL10Gold cells for sequencing and yeast retransformation. The number of mutations varied from three in MV1 and MV3 to five in MV2 (**Table 1**). All mutation sites were located on the protein surface, four in loops and nine in helices (**Fig. 5**). Surface mutations with beneficial effects on activity and stability have previously been reported for several enzymes including VP [33, 50, 51]. Two mutations were located close to the catalytic Trp164 residue essential for VP activity. Mutant MV1 featured three substitutions: Ala32Glu, Leu124His and Val163Asp. Val163Asp was located near Trp164 and increased the

negative charge in the area, which may promote Trp cation radical stabilization [9,10]. The introduction of polar and/or charged surface amino acid residues, such are all three substitution we detected in MV1 and Leu268Glu mutation detected in MVP2, also increased the thermal stability and oxidative stability of LiP [33, 51]. These mutations are increasing enzymes solubility in polar solvents, and may form new bonds with both solvent and other residues in protein structure, leading to protein stabilization. Additionally, these mutations are often detected as a result of enzymes directed evolution for stability improvement experiments, due to their low effect on enzyme activity [33, 52-54]. Mutant MV2 featured five substitutions: Pro90Gly, Ala108Thr, Val109Ala, Gln196Gly and Leu268Glu, with only Leu268Glu located in a loop and the others in helices. The Gln196Gly mutation was near the Ca^{2+}-binding site [52]. The presence of Ca^{2+} in ligninolytic peroxidases stabilizes the histidine residue involved in heme coordination, and the replacement of a bulky amino acid with a small one such as Gly might lead to relaxation of the region and facilitate the coordination of this cation. Mutations in surfacely located loops such are Leu268Glu detected in MV2 variant and Ala132Glu in ML1 variant and two out of three substitutions featured by MV3 variant, Gly51Ala, Ile181Thr proven to have beneficial effects on oxidative, thermal stability and stability in organic solvents for various enzymes. These mutations also had the lowest negative influence on enzyme activity. Additionally, mutations detected in surfacely located helixes may lead to a slight reposition of nearby residues and facilitate formation of new stabilizing interactions [38, 53, 54]. Mutant MV3 featured three substitutions: Gly51Ala, Ile181Thr and Met247Leu. The last of these was located close to Trp164 (3.7 Å) [55]. Met residues are easily oxidized, and the rational design of VP variants with greater oxidative stability has already been shown to benefit from the replacement of Met [45, 55]. The same was observed for other peroxide dependent enzymes such are manganese peroxidase and glucose oxidase [52, 56]. It was reported that mutation Met247Leu improves oxidative stability of VP

[45], but also that mutation Met247Phe has no impact on oxidative stability of the same enzyme [55]. Therefore, we cannot be sure if enzyme's oxidative stability was improved due to removal of easily oxidized Met residue, or due to substitution near to catalytic Trp164 residue. Additionally, from obtained results, we can not conclude if all introduced mutations have impact on VP's stability and/or activity.

Table 1. The substation mutations detected in the selected VP variants.

VP variant	Mutation 1	Mutation 2	Mutation 3	Mutation 4	Mutation 5
MV1	Ala132Glu	Leu124His	Val163Asp	×	×
MV2	Pro90Gly	Ala108Thr	Val109Ala	Gln196Gly	Leu268Glu
MV3	Gly51Ala	Ile181Thr	Met247Leu	×	×

Since, one of broad VP application possibilities is degradation and removal of toxic and cancerogenic azo-dyes from environment, we tested our system for these purposes, along with assessing the reusability of the VP variants, which is usually achieved by immobilization [57], by following degradation of azo-dye Reactive black 5 [58, 59]. Yeast cell wall fragments coated with wtVP or the three selected variants were therefore tested in multiple cycles for their ability to degrade the azo dye Reactive Black 5 (**Fig. 6B**). After each cycle of 12 h, the cell wall fragments were washed and reused with a fresh dye/H_2O_2 mixture. The activity of wtVP decreased moderately over the 10 reaction cycles to ~70% of the initial value, whereas the activity of MV1 decreased only to ~90% of the initial value, and MV2 and MV3 showed almost no loss of activity at all. These results suggested that the three variants show greater oxidative stability than wtVP and could be suitable for bioremediation applications.

3.5 Purification and kinetic characterization of Aga2-VP fusion proteins

The three VP variants (and wtVP) were extracted from the yeast cell wall preparations by incubating with 2-mercaptoethanol, which disrupts the disulfide bonds between Aga1 and the

Aga2-VP fusion proteins [44]. After buffer exchange, the extracted Aga2-VP proteins were purified by ion exchange chromatography and eluted with 300 mM NaCl (**Fig. S6**). Purity was confirmed by gel electrophoresis under native conditions followed by zymography. The single bands on the native gel (**Fig. S7A**) matched the active zones on the zymography gel with guaiacol and H_2O_2 as substrates (**Fig. S7B**). A slightly broader bands reveled after zymography may be a consequence of reaction product diffusion [44]. The molecular weight of the isolated Aga2-wtVP was determined by SDS-PAGE, revealing a broad band of 50–65 kDa (**Fig. S8**). This was higher than the theoretical molecular weight of 51.5 kDa, based on the combined 42 kDa molecular weight of wtVP [4] and 9.5 kDa molecular weight of Aga2 [44]. Similar broad bands have been detected for many recombinant proteins produced in *S. cerevisiae*, including an Aga2-glucose oxidase fusion protein (100–140 kDa), which was also higher in molecular weight than expected when confirmed by gel filtration [44]. The difference in size may reflect a combination of microheterogeneity and the presence of additional glycan groups on proteins secreted by *S. cerevisiae*, as observed for the enzyme invertase with an empirical molecular weight of 60–120 kDa [60]. Also, even though native electrophoresis was run till bromophenol blue was at the end of the gel, high position of protein bands on native electrophoresis may be a result of both hyperglycosylation and enzyme oligomerization via Aga2 protein under native conditions [44].

Table 2. Kinetic characteristics of the Aga2-wtVP fusion protein and three selected variants.

	wtVP	MV1	MV2	MV3
k_{cat} (s^{-1})	0.89±0.04	1.32±0.03	1.11±0.05	0.76±0.02
K_m (mM)	0.28±0.01	0.92±0.03	0.65±0.03	0.24±0.01
k_{cat}/K_m ($s^{-1}mM^{-1}$)	3.18±0.23	1.43±0.06	1.71±0.07	3.17±0.04

It was reported that substitution of Met247Leu led to almost 2-fold decrease in both k_{cat} and K_m values for H_2O_2, resulting in a very similar specificity constant to the wtVP [45]. MV3 variant, featuring the same mutation, shown slight decrease in both parameters, also resulting in a very similar specificity constant to the wtVP (Table 2). Additionally, MV3 variant features two more mutations those can have impact on enzymes reactivity with H_2O_2. This effect on kinetic parameters and VP activity can be a result of mutation effect on LRET pathway, due to its close proximity to Trp164 [33]. However, both MV1 and MV2 showed higher K_m values for H_2O_2 than wtVP, 3.3-fold higher in the case of MV2 and 2.3-fold for MV3. Additionally, both MV1 and MV2 showed higher k_{cat} values than the wtVP (1.48 and 1.25-fold). However, changes in k_{cat} and K_m parameters for both MV1 and MV2 resulted in lower than wtVP specificity constant for H_2O_2 (2.22-fold for MV1 and 1.86-fold for MV2). Similar increases in K_m values were observed for manganese peroxidase mutants with greater oxidative stability, indicating that stabilization may in some cases correspond to the enzyme's lower reactivity with H_2O_2, and therefore, lower inactivation rate [51].

4. Conclusions

In this study, we developed the first high-throughput screening system for the selection of VP variants with higher oxidative stability. This was achieved by exploiting libraries of enzyme variants displayed on the surface of yeast cells and using a one-step TyrF-based assay without compartmentalization. We initially confirmed the efficiency of our approach by sorting reference libraries, and found that the 5% library achieved a 13.8-fold enrichment of positive clones. After two rounds of sorting, the proportion of yeast cells expressing VP variants with higher oxidative stability compared to wtVP increased from 1% to 56%, confirming the efficiency of the method using real libraries. Three of the most stable mutants were characterized in greater detail,

revealing the presence of 3–5 mutations located on the enzyme surface. All three variants showed greater oxidative stability than wtVP, retaining up to 70% of their activity after 1 h pre-incubation in 30 mM H_2O_2 compared to the complete loss of wtVP activity after 50 min pre-incubation. Two of the three variants retained full activity after 10 dye degradation cycles and the other lost only 10% of its initial activity, whereas the activity of wtVP declined by ~30%. Kinetic analysis suggested that the three variants use different mechanisms for stabilization, which do not necessarily affect the reduction of H_2O_2. Since, the cell sorting resulted in significant enrichment of population expressing the VP variants with higher than wtVP oxidative stability and since we were able to isolate and characterize VP variants with higher residual activity than wtVP after incubation in H_2O_2, obtained results suggest that the developed screening system may be used for improvement of VP characteristics important for its applications.

Competing interests

The authors declare no competing financial interests.

Acknowledgements

The authors would like to thank Professor Dane Wittrup, Massachusetts Institute of Technology, for providing the pCTCON2 vector and *S. cerevisiae* EBY100 competent cells, and Dr. Helga Schinkel, Fraunhofer IME (Aachen, Germany) for valuable discussion. This work was supported by funds from the Ministry of Education, Science and Technological Development, Republic of Serbia via project numbers ON172049, ON173017 and III46010.

References

[1] A.T. Smith, N.C. Veitch, Substrate binding and catalysis in hem peroxidases. Curr. Opin. Chem. Biol. 2 (1998) 269-278. https://doi.org/10.1016/S1367-5931(98)80069-0

[2] M. Hofrichter, R. Ullrich, M.J. Pecyna, C. Liers, T. Lundell, New and classic families of secreted fungal heme peroxidases. Appl. Microbiol. Biotechnol. 87 (2010) 871–897. https://doi.org/10.1007/s00253-010-2633-0

[3] T. Mester, J.A. Field, Characterization of a novel manganese peroxidase-lignin peroxidase hybrid isozyme produced by *Bjerkandera* species strain BOS55 in the absence of manganese. J. Biol. Chem. 273 (1998) 15412-15417. https://doi.org/10.1074/jbc.273.25.15412

[4] F.J. Ruiz-Dueñas, M.J. Martínez, A.T. Martínez, Molecular characterization of a novel peroxidase isolated from the ligninolytic fungus *Pleurotus eryngii*. Mol. Microbiol. 31 (1999) 223-235. https://doi.org/10.1046/j.1365-2958.1999.01164.x

[5] F.J. Ruiz-Dueñas, M. Morales, E. García, Y. Miki, M.J. Martínez, A.T. Martínez, Substrate oxidation sites in versatile peroxidase and other basidiomycete peroxidases. J. Exp. Bot. 60 (2009) 441–452. https://doi.org/10.1093/jxb/ern261

[6] M. Ayala-Aceves, M.C. Baratto, R. Basosi, R. Vázquez-Duhalt, R. Pogni, Spectroscopic characterization of a manganese–lignin peroxidase hybrid isozyme produced by *Bjerkandera adusta* in the absence of manganese: evidence of a protein-centred radical by hydrogen peroxide. J. Mol. Cat. B: Enzym. 16 (2001) 159–167. https://doi.org/10.1016/S1381-1177(01)00056-X

[7] F.J. Ruiz-Dueñas, R. Pogni, M. Morales, S. Giansanti, M.J. Mate, A. Romero, M.J. Martínez, R. Basosi, A.T. Martínez, Protein radicals in fungal versatile peroxidase: catalytic tryptophan radical in both Compound I and Compound II and studies on W164Y, W164H and W164S variants. J. Biol. Chem. 284 (2009) 7986–7994. https://doi.org/10.1074/jbc.M808069200

[8] F.J. Ruiz-Dueñas, M. Morales, M.J. Mate, A. Romero, M.J. Martínez, A.T. Smith, A.T. Martínez, Site-directed mutagenesis of the catalytic tryptophan environment in *Pleurotus eryngii* versatile peroxidase. Biochemistry 47 (2008) 1685–1695. https://doi.org/10.1021/bi7020298

[9] F.J. Ruiz-Dueñas, M. Morales, M. Pérez-Boada, T. Choinowski, M.J. Martínez, K. Piontek, A.T. Martínez, Manganese oxidation site in Pleurotus eryngii versatile peroxidase: a site-directed mutagenesis, kinetic and crystallographic study. Biochemistry 46 (2007) 66-77. https://doi.org/10.1021/bi061542h

[10] M. Pérez-Boada, F.J. Ruiz-Dueñas, R. Pogni, R. Basosi, T. Choinowski, M.J. Martínez, K. Piontek, A.T. Martínez, Versatile peroxidase oxidation of high redox potential aromatic compounds: site-directed mutagenesis, spectroscopic and crystallographic investigations of three long-range electron transfer pathways. J. Mol. Biol. 354 (2005) 385–402. https://doi.org/10.1016/j.jmb.2005.09.047

[11] P.R. Moreira, E. Almeida-Vara, F.X. Malcata, J.C. Duarte, Lignin transformation by a versatile peroxidase from a novel Bjerkandera sp strain. Int. Biodeterior. Biodegrad. 59 (2007) 234–238. https://doi.org/10.1016/j.ibiod.2006.11.002

[12] D. Salvachúa, A. Prieto, M.L. Mattinen, T. Tamminen, T. Liitiä, M. Lille, S. Willför, A.T. Martínez, M.J. Martínez, C.B. Faulds, Versatile peroxidase as a valuable tool for generating new biomolecules by homogeneous and heterogeneous cross-linking. Enz. Microb. Tech. 52 (2013) 303-311. https://doi.org/10.1016/j.enzmictec.2013.03.010

[13] E. de Jong, J.A. Field, J.A.F.M. Dings, J.B.P.A. Wijnberg, J.A.M. de Bont, De novo biosynthesis of chlorinated aromatics by the white-rot fungus *Bjerkandera* sp BOS55. Formation of 3-chloro-anisaldehyde from glucose. FEBS Lett. 305 (1992) 220-224. https://doi.org/10.1016/0014-5793(92)80672-4

[14] Y.X. Wang, R. Vázquez-Duhalt, M.A. Pickard, Manganese-lignin peroxidase hybrid from *Bjerkandera adusta* oxidizes polycyclic aromatic hydrocarbons more actively in the absence of manganese. Can. J. Microbiol. 49 (2003) 675-682. https://doi.org/10.1139/w03-091

[15] E. Rodríguez, O. Nuero, F. Guillén, A.T. Martínez, M.J. Martínez, Degradation of phenolic and non-phenolic aromatic pollutants by four *Pleurotus* species: the role of laccase and versatile peroxidase. Soil. Biol. Biochem. 36 (2004) 909–916. https://doi.org/10.1016/j.soilbio.2004.02.005

[16] I.E. Touahar, L. Haroune, S. Ba, J.P. Bellenger, H. Cabana, Characterization of combined cross-linked enzyme aggregates from laccase, versatile peroxidase and glucose oxidase, and their utilization for the elimination of pharmaceuticals. Sci. Tot. Environ. 481 (2014) 90-99. https://doi.org/10.1016/j.scitotenv.2014.01.132

[17] G. Davila-Vazquez, R. Tinoco, M.A. Pickard, R. Vazquez-Duhalt, Transformation of halogenated pesticides by versatile peroxidase from *Bjerkandera adusta*. Enz. Microb. Tech. 36 (2005) 223-231. https://doi.org/10.1016/j.enzmictec.2004.07.015

[18] K.S. Siddiqui, H. Ertan, T. Charlton, A. Poljak, A.K.D. Khaled, X. Yang, G. Marshall, R. Cavicchioli, Versatile peroxidase degradation of humic substrates: Use of isothermal titration calorimetry to assess kinetics, and applications to industrial waste. J. Biotech. 178 (2014) 1-11. https://doi.org/10.1016/j.jbiotec.2014.03.002

[19] M. Hibi, S. Hatahira, M. Nakatani, K. Yokozeki, S. Shmizu, J. Ogawa, Extracellular oxidases of *Cerrena* sp. complementary functioning in artificial dye decolorization including laccase, manganese peroxidase, and novel versatile peroxidases. Biocat. Agricul. Biotech. 1 (2012) 220-225. https://doi.org/10.1016/j.bcab.2012.03.003

[20] P.J. Harvey, H.E. Schoemaker, J.M. Palmer, Veratryl alcohol as a mediator and the role of radical cations in lignin biodegradation by *Phanerochaete chrysosporium*. FEBS Lett. 195 (1986) 242-246. https://doi.org/10.1016/0014-5793(86)80168-5

[21] R. Tinoco, J. Verdín, R. Vázquez-Duhalt, Role of oxidizing mediators and tryptophan 172 in the decoloration of industrial dyes by the versatile peroxidase from *Bjerkandera adusta*. J. Mol. Catal. B: Enzym. 46 (2007) 1-7. https://doi.org/10.1016/j.molcatb.2007.01.006

[22] A. Khindaria, I. Yamazaki, S.D. Aust, Stabilization of the veratryl alcohol cation radical by lignin peroxidase. Biochemistry 35 (1996) 6418-6424. https://doi.org/10.1021/bi9601666

[23] H. Kamitsuji, T. Watanabe, Y. Honda, M. Kuwahara, Direct oxidation of polymeric substrates by multifunctional manganese peroxidase isozyme from *Pleurotus ostreatus* without redox mediators. Biochem. J. 386 (2005) 387-393. https://doi.org/10.1042/BJ20040968

[24] H. Wariishi, M.H. Gold, Lignin peroxidase compound III. Mechanism of formation and decomposition. J. Biol. Chem. 265 (1990) 2070–2077.

[25] A.N. Hiner, J. Hernández-Ruíz, J.N. Rodríguez-López, F. Garcia-Canovas, N.C. Brisset, A.T. Smith, et al., Reactions of the class II peroxidases, lignin peroxidase and *Arthromyces ramosus* peroxidase, with hydrogen peroxide. Catalase-like activity, compound III formation, and enzyme inactivation. J. Biol. Chem. 277 (2002) 26879–26885. https://doi.org/10.1074/jbc.M200002200

[26] B. Valderrama, M. Ayala, R. Vázquez-Duhalt, Suicide inactivation of peroxidases and the challenge of engineering more robust enzymes. Chem. Biol. 9 (2002) 555–565. https://doi.org/10.1016/S1074-5521(02)00149-7

[27] T. Mastuura, T. Yomo, In vitro evolution of proteins. J. Biosci. Bioeng. 101 (2006) 449-456. https://doi.org/10.1263/jbb.101.449

[28] Q. Liu, G. Xun, Y. Feng, The state-of-the-art strategies of protein engineering for enzyme stabilization, Biotechnol. Adv. 37 (2019) 530-537. https://doi.org/10.1016/j.biotechadv.2018.10.011

[29] H. Leemhuis, W. Stein, A.D. Griffiths, F. Hollfelder, New genotype-phenotype linkages for directed evolution of proteins. Curr. Opin. Struct. Biol. 15 (2005) 472-478. https://doi.org/10.1016/j.sbi.2005.07.006

[30] M.S. Packer, D.R. Liu, Methods for directed evolution of proteins. Nat. Rev. Genet. 16 (2015) 379-394. https://doi.org/10.1038/nrg3927

[31] A. Aharoni, G. Amatai, K. Bernath, S. Magdassi, D.S. Tawfik, High-throughput screening of enzyme libraries. Chem. Biol. 12 (2005) 1281-1289. https://doi.org/10.1016/j.chembiol.2005.09.012

[32] E. Garcia-Ruiz, D. Gonzalez-Perez, F. J. Ruiz-Dueñas, A. T. Martínez, M. Alcalde, Directed evolution of a temperature-, peroxide- and alkaline pH-tolerant versatile peroxidase. Biochem. J. 441 (2012) 487-498. https://doi.org/10.1042/BJ20111199

[33] K. Rye, S. Y. Hwang, K. H. Kim, J. H. Kang, E. K. Lee, Functionality improvement of fungal lignin peroxidase by DNA shuffling for 2,4-dichlorophenol degradability and H_2O_2 stability. J. Biotech. 133 (2008) 110-115. https://doi.org/10.1016/j.jbiotec.2007.09.008

[34] G.M. Cherf, J.R. Cochran, Applications of yeast surface display for protein engineering. Methods Mol. Biol. 1319 (2015) 155-175. https://doi.org/10.1016/j.micres.2016.12.002

[35] S.A. Gai, K.D. Wittrup, Yeast surface display for protein engineering and characterization. Curr. Oppin. Struct. Biol. 17 (2007) 467-473. https://doi.org/10.1016/j.sbi.2007.08.012

[36] A. Kondo, M. Ueda, Yeast cell-surface display – applications of molecular display. Appl. Microbiol. Biotechnol. 64 (2004) 28-40. https://doi.org/10.1007/s00253-003-1492-3

[37] E.T. Boder, K.D. Wittrup, Yeast surface display for directed evolution of protein expression, affinity and stability. Methods Enzimol. 328 (2000) 430-444. https://doi.org/10.1016/S0076-6879(00)28410-3

[38] E.T. Boder, K.D. Wittrup, Yeast surface display for screening combinational polypeptide libraries. Nat. Biotechnol. 15 (1997) 553-557. https://doi.org/10.1038/nbt0697-553

[39] A.H.N. Hopman, F.C.S. Ramaekers, E.J.M. Speel, Rapid synthesis of biotin-, digoxigenin-, trinitrophenil-, and uorochrome-labeled tyramides and their application for in situ hybridization using CARD amplification. J. Histochem. Cytochem. 46 (1998) 771-777. https://doi.org/10.1177/002215549804600611

[40] K. Miyazaki, M. Takenouchi, Creating random mutagenesis libraries using megaprimer PCR of whole plasmid. Biotech. 33 (2002) 1033–1038. https://doi.org/10.2144/02335st03

[41] R.D. Gietz, R.H. Schiestl, High-efficiency yeast transformation using the LiAc/SS carrier DNA/PEG method. Nat. Protoc. 2 (2007) 31-34. https://doi.org/10.1038/nprot.2007.13

[42] D. Lipovesk, E. Antipov, K.A. Amstrong, M.J. Olsen, et al., Selection of horseradish peroxidase variants with enhanced enantioselectivity by yeast surface display. Chem. Biol. 14 (2007) 1176-1185. https://doi.org/10.1016/j.chembiol.2007.09.008

[43] M.V. Singh, P.A. Weil, A method for plasmid purification directly form yeast. Anal. Biochem. 307 (2002) 13-17. https://doi.org/10.1016/S0003-2697(02)00018-0

[44] M. Blazić, G. Kovačević, O. Prodanović, R. Ostafe, M. Gavrović-Jankulović, R. Fischer, R. Prodanović, Yeast surface display for the expression, purification and characterization of wild-type and B11 mutant glucose oxidases. Prot. Expr. Pur. 89 (2013) https://doi.org/175-180. 10.1016/j.pep.2013.03.014

[45] X. Bao, X. Haung, Improvement of hydrogen peroxide stability of *Pleurotus eryngii* versatile ligninolytic peroxidase by rational protein engineering. Enz. Microb. Tech. 54 (2014) 51-58. https://doi.org/10.1016/j.enzmictec.2013.10.003

[46] G. Kovačević, R. Ostafe, A. M. Balaž, R. Fischer, R. Prodanović, Development of GFP-based high-throughput screening system for directed evolution of glucose oxidase. J. Biosci. Bioeng. 127 (2018) 30-37. https://doi.org/10.1016/j.jbiosc.2018.07.002

[47] R. Ostafe, R. Prodanovic, J. Nazor, R. Fischer, Ultra-High-Throughput Screening Method for the Directed Evolution of Glucose Oxidase. Chem. Biol. 21 (2014) 414-421. https://doi.org/10.1016/j.chembiol.2014.01.010

[48] R. Ostafe, R. Prodanovic, U. Commandeur, R. Fischer, Flow cytometry-based ultra-high-throughput screening assay for cellulase activity. Anal. Biochem. 435 (2013) 93-98. https://doi.org/10.1016/j.ab.2012.10.043

[49] R. Prodanovic, R. Ostafe, M. Blanusa, U. Schwaneberg, Vanadium bromoperoxidase-coupled fluorescent assay for flow cytometry sorting of glucose oxidase gene libraries in double emulsions. Anal. Bioanal. Chem. 404 (2012) 1439-1447. https://doi.org/10.1007/s00216-012-6234-x

[50] C. A. Voigt, S. L. Mayo, F. H. Arnold, Z. G. Wang, Computational method to reduce the search space for directed protein evolution. Proc. Natl. Acad. Sci. 98 (2001) 3778-3783. https://doi.org/10.1073/pnas.051614498

[51] C. Miyazaki, H. Takahashi, Engineering of the H_2O_2-binding pocket region of a recombinant manganese peroxidase to be resistant to H_2O_2. FEBS lett. 509 (2001) 111-114. https://doi.org/10.1016/S0014-5793(01)03127-1

[52] Y. Semba, M. Ishida, S. Yokobori, A. Yamadishi, Ancestral amino acid substitution improves the thermal stability of recombinant lignin peroxidase from white-rot fungi, *Phanerochaete chrysosporium* strain UAMH 3641. Prot. Engin. Des. Selec. 28 (2015) 221–230. https://doi.org/10.1093/protein/gzv023

[53] F. Zhu, B. He, H. Deng, C. Chen, W. Wang, N. Chen, Improvement in organic solvent resistance and activity of metalloprotease by directed evolution. J. Biotechnol. 309 (2020) 68-74. https://doi.org/10.1016/j.jbiotec.2019.12.014

[54] Z. Emruzi, S. Aminzadeh, A. A. Karkhane, J. Alikhajeh, K. Hagjbeen, D. Gholami, Improving the thermostability of *Serratia marcescens* B4A chitinase *via* G191V site-directed mutagenesis. Int. J. Biol. Macromol. 116 (2018) 64-70. https://doi.org/10.1016/j.ijbiomac.2018.05.014

[55] V. Sáez-Jiménez, S. Acebes,V. Guallar, A. T.Martínez, F. J.Ruiz-Dueñas, Improving the oxidative stability of a high redox potential fungal peroxidase by rational design, PLOS ONE, 10 (2015) e0124750. https://doi:10.1371/journal.pone.0124750

[56] G. Kovačević, R. Ostafe, R. Fischer, R. Provanović, Influence of methionine residue position on oxidative stability of glucose oxidase from *Aspergillus niger*. Biochem. Eng. J. 146 (2019) 143-149. https://doi.org/10.1016/j.bej.2019.03.016

[57] S. Datta, L. R. Christena, Y. R. S. Rajaram, Enzyme immobilization: an overview on techniques and support materials. Biotech. 3 (2013) 1−9. https://doi.org/10.1007/s13205-012-0071-7

[58] R. Ilamathi, A. Merline Sheela, N. Nagendra Gandhi, Comparative evaluation of *Pseudomonas* species in single chamber microbial fuel cell with manganese coated cathode for reactive azo dye removal. Int. Biodeter. Biodegr. , 144 ,(2019) 104744. https://doi.org/10.1016/j.ibiod.2019.104744

[59] B. C. Ventura-Camargo, M. A. Marin-Morales, Azo dyes: characterization and toxicity-A review. TLIST, 2 (2013) 85-103.

[60] F.K. Chu, F. Maley, The effect of glucose on the synthesis and glycosylation of the polypeptide moiety of yeast external invertase, J. Biol. Chem. 255 (1980) 6392–6397.

Figure captions

Figure 1. Summary of the experimental workflow. The *P. eryngii* wtVP gene was inserted into the pCTCON2 vector. The resulting construct was used as a template for preparation of random mutagenesis libraries with different mutation rates. The wtVP and VP variant libraries were expressed on the yeast cell surface. Cells expressing the VP libraries were used for flow cytometry-based sorting to select for increased oxidative stability. The cells were incubated in 30 mM H_2O_2, washed and used for the TyrF reaction in presence of 1 mM H_2O_2. After washing, the cells were gated on FITC/forward scatter plots and the most active cells (cells with the brightest green fluorescence) after incubation in 30 mM H_2O_2 were sorted and recovered. Sorting was repeated after the incubation of previously sorted cells in 30 mM H_2O_2 (blue arrows). After recovery on YNB-CAA plates, selected VP variants were expressed in microtiter plates and screened for the highest activity after incubation in 30 mM H_2O_2. The most stable variants were sequenced and characterized.

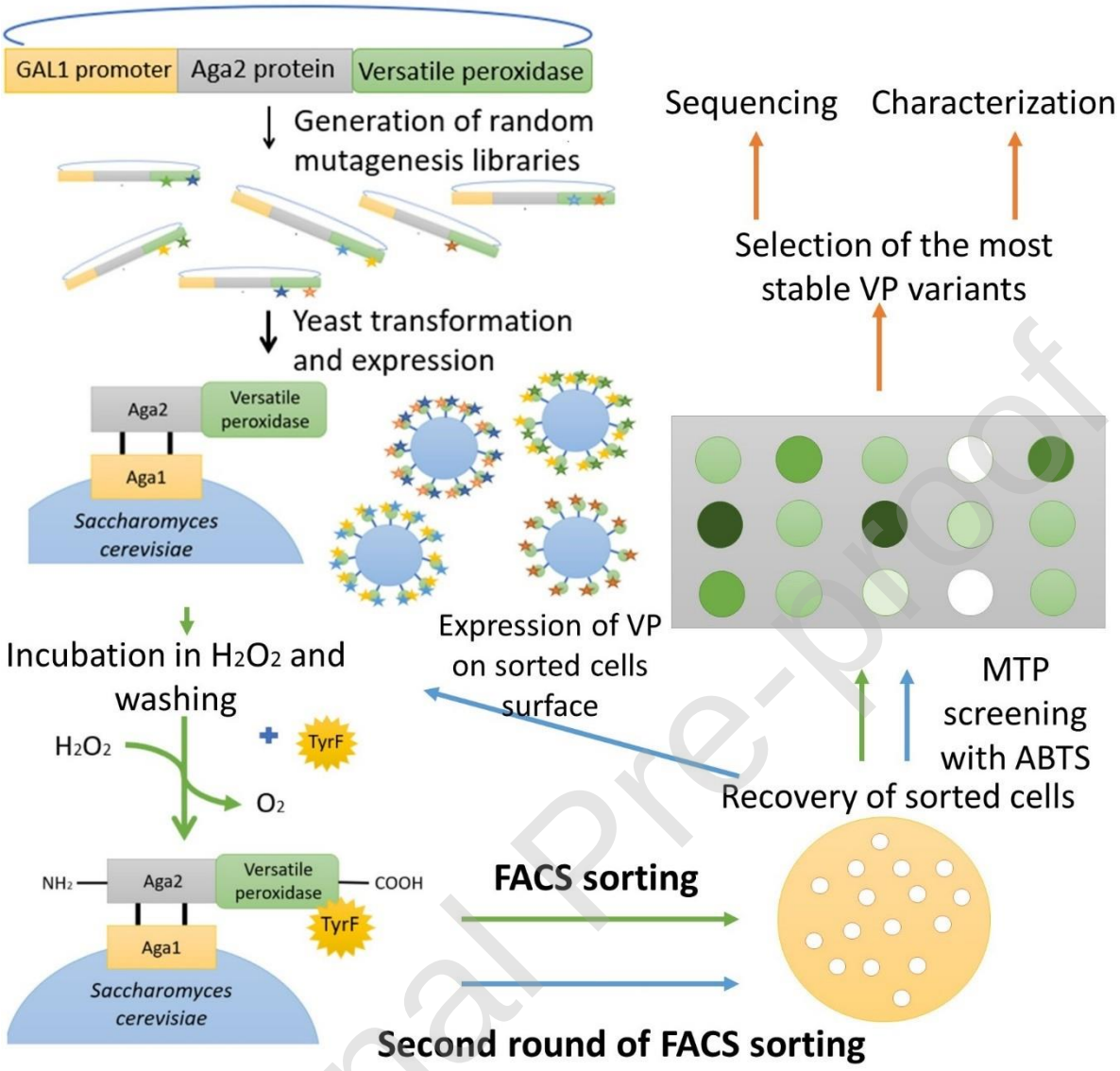

Figure 2. Preparation of reference libraries. (A) FACS recordings of reference libraries comprising different proportions of cells expressing wtVP mixed with cells transformed with the empty vector. The reference libraries were combined with assay components (TyrF and H_2O_2) and incubated for 1 min. After a series of washing steps, 10^4 cells were analyzed by FACS. The bivariate histograms show the correlation between FITC (VP activity) and forward scatter (cell size). The percentages above the histograms indicate the theoretical proportion of cells expressing active VP in the reference libraries. (B) Enrichment of reference libraries by FACS. Positive cells were gated by comparing 100% positive and 0% positive mixes. Four hundred cells were sorted in single-cell mode for

every mix, and ~300 cells were recovered on agar plates. After incubation, the cells were seeded into microtiter plates and VP activity was measured using an ABTS assay.

A

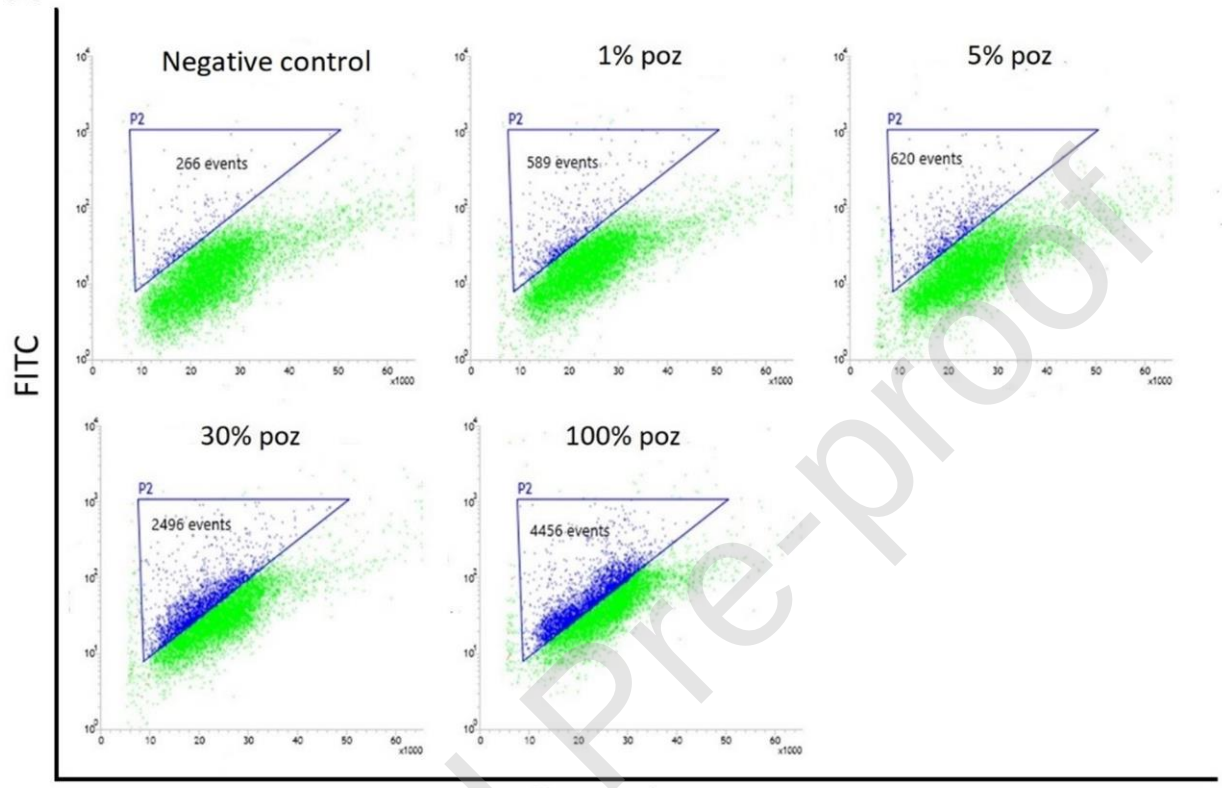

B

Reference mix name	Ref1	Ref2	Ref3
Before sorting	1%	5%	30%
After sorting	37.8±1.9%	68.9±2.0%	46.7±3.4%

Figure 3. Stability of VP variants in H_2O_2. FACS recordings (A) before pre-incubation in H_2O_2 and (B) after 20 min pre-incubation in 30 mM H_2O_2, showing negative control cells (cells transformed with the empty vector) and cells expressing wtVP after reacting with TyrF for 1 min. After a series of washing steps, cells were incubated with TyrF and 1 mM H_2O_2 for 1 min and washed again before FACS analysis. The bivariate histograms show the correlation between FITC (VP activity) and forward scatter (cell size) for a total of 10^4 of cells. Gates (P2) were set

based on the difference between positive and negative control cells and represent the fraction of active cells after incubation with H_2O_2.

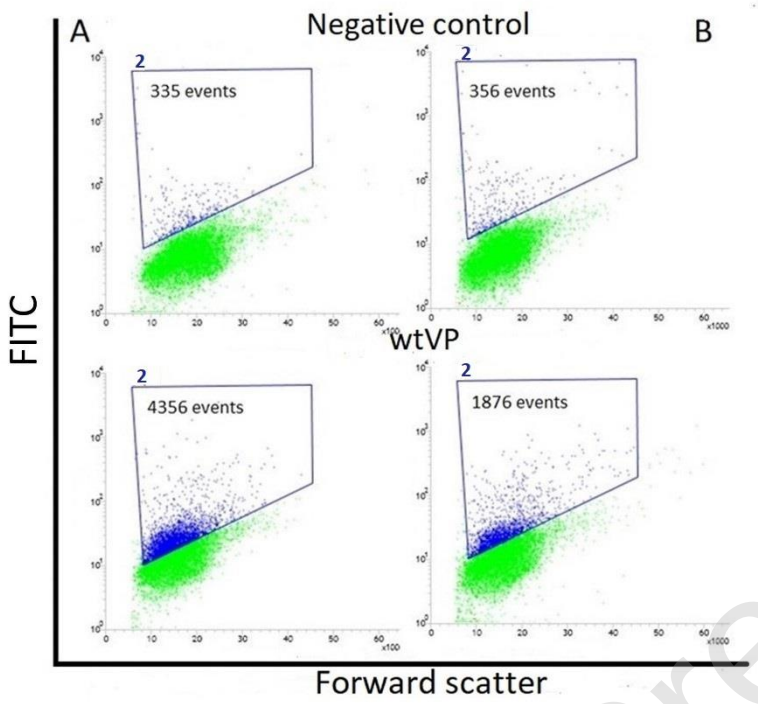

Figure 4. Multiple sorting rounds. (A) FACS recordings of the VP random mutagenesis library before and during two rounds of sorting, based on a reaction with TyrF for 1 min. The bivariate histograms show the correlation between FITC (VP activity) and forward scatter (cell size) for a total of 10^4 cells. (B) FACS recordings (10^4 cells) of the VP random mutagenesis library before and during two rounds of sorting after incubation in 30 mM H_2O_2 for 20 min. Gates were set based on the difference between positive and negative cells (Figure 2). (C) Activity profiles represent the oxidative stability of 300 randomly picked cells before and after the first and second rounds of library sorting compared to wtVP as determined in an ABTS microtiter plate assay. Legend: Gray portion – The cells expressing variants with oxidative stability equal to wtVP; Yellow portion - The cells expressing variants with oxidative stability lower than wtVP; Orange portion - The cells expressing variants without VP activity (Ten times lower activity with ABTS as a substrate than wtVP); Blue portion - The cells expressing variants with oxidative stability higher than wtVP.

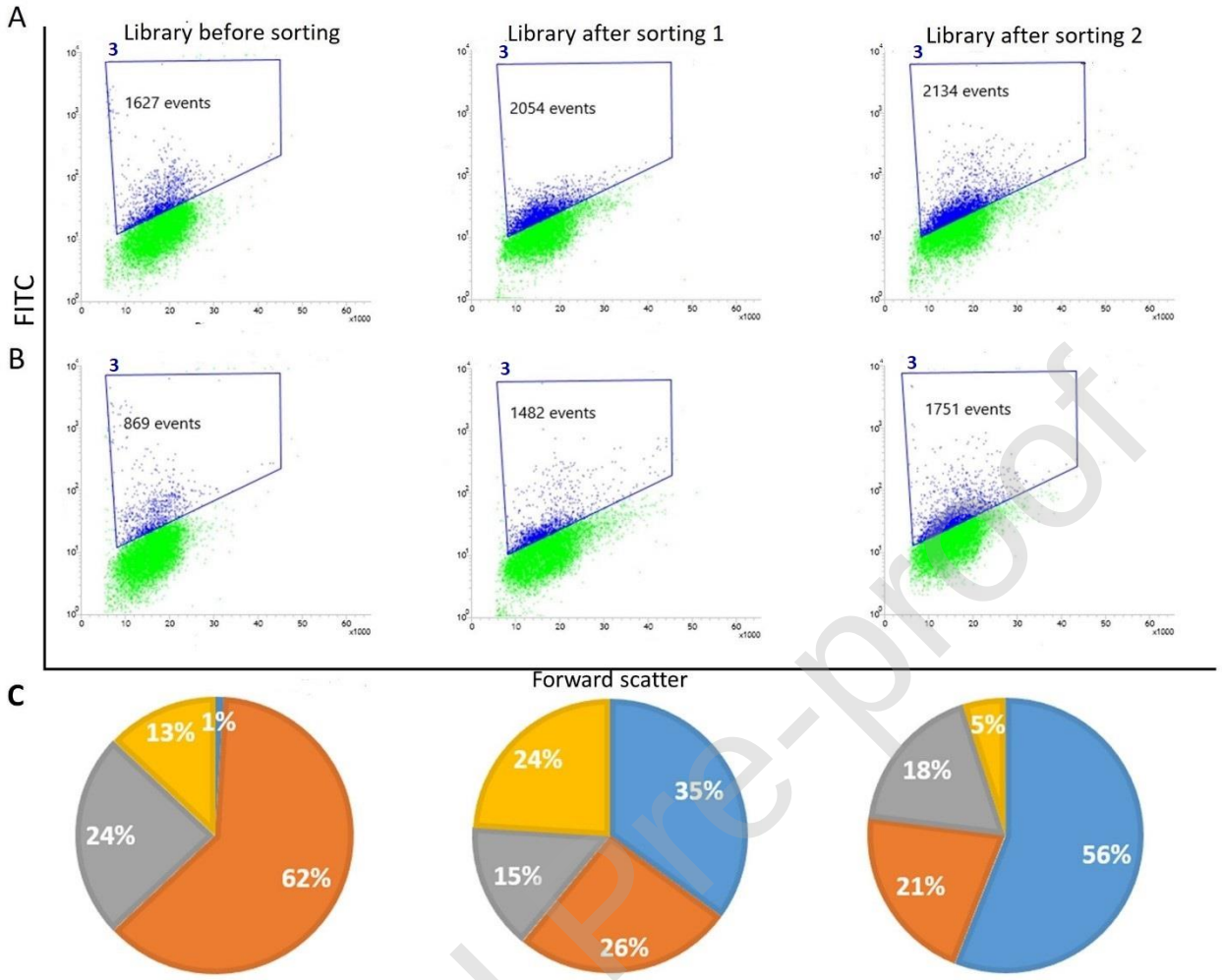

Figure 5. A ribbon diagram of the three-dimensional structure of VP (A) Positions of amino acid substitutions detected in the three best-performing VP variants. Key: magenta – MV1, blue – MV2, red – MV3. (B) Residues near to H_2O_2 binding pocket. (C) Residues included in coordination of distal Ca^{2+}. (D) Residues included in coordination of proximal Ca^{2+}.

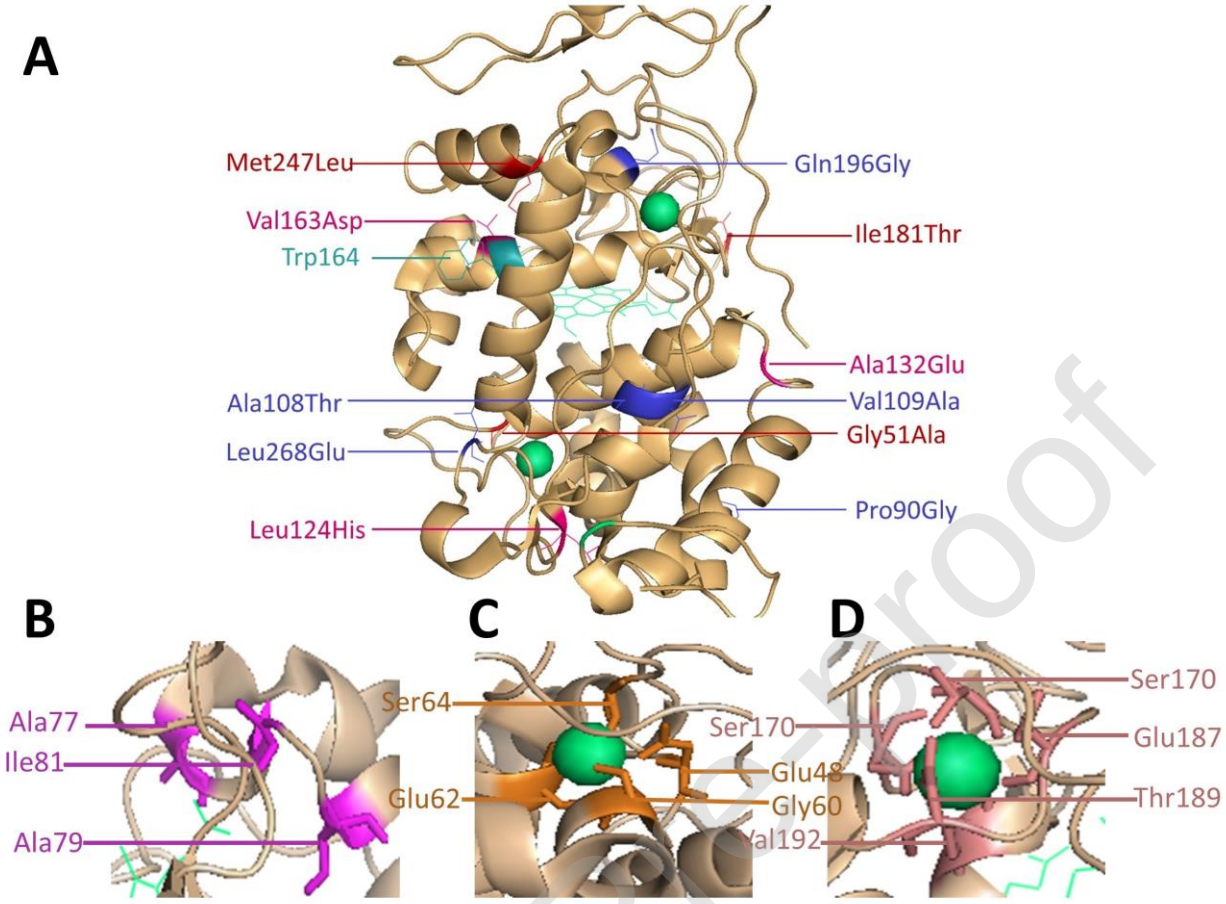

Figure 6. Characterization of wtVP and selected variants (A) Residual activity of wtVP and selected VP variants after incubation in H_2O_2. The graph shows the declining activity of wtVP (blue), MV1 (yellow), MV2 (orange) and MV3 (gray) incubated in 30 mM H_2O_2 as determined in an ABTS microtiter plate assay. Data are means of triplicate experiments with error bars indicating standard error. Error bars are not visible when smaller than the symbol size. (B) Multiple degradation cycles of Reactive Black 5. Dye degradation was followed for 10 cycles, each 12 h in duration, using VP-coated yeast cell wall fragments. After each cycle cell, the wall fragments were washed with reaction buffer and mixed with fresh dye/H_2O_2 solution. Key: wtVP (blue), MV1 (yellow), MV2 (orange) and MV3 (gray). Data are means of triplicate experiments with error bars indicating standard error. Error bars are not visible when smaller than the symbol size.

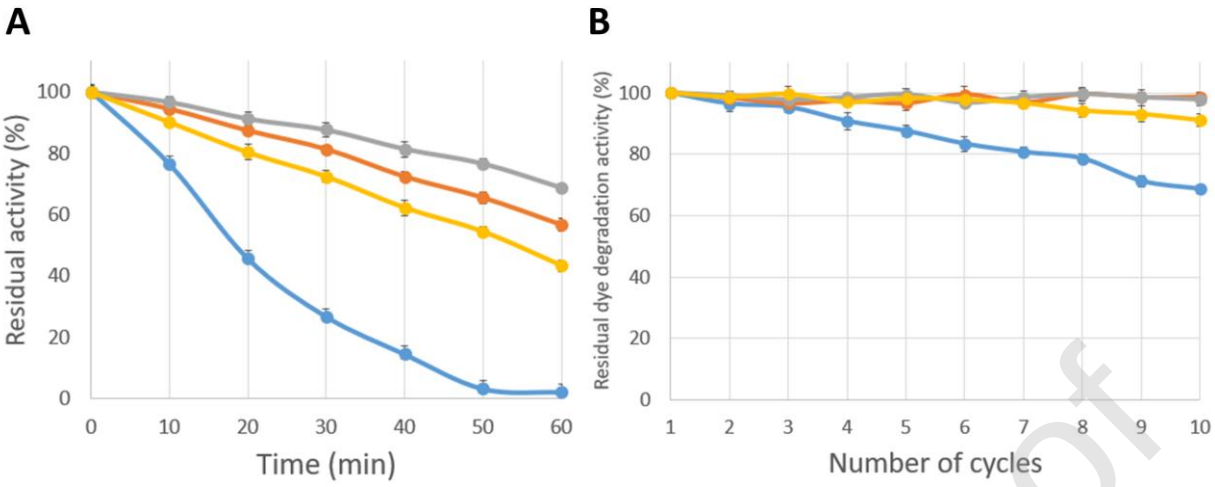

Table 1. Introduced amino acid mutations in selected VP variants.

VP variant	Mutation 1	Mutation 2	Mutation 3	Mutation 4	Mutation 5
MV1	Ala132Glu	Leu124His	Val163Asp	×	×
MV2	Pro90Gly	Ala108Thr	Val109Ala	Gln196Gly	Leu268Glu
MV3	Gly51Ala	Ile181Thr	Met247Leu	×	×

Table 2. Kinetic characteristics of the Aga2-wtVP fusion protein and three selected variants.

	wtVP	MV1	MV2	MV3
k_{cat} (s^{-1})	0.89±0.04	1.32±0.03	1.11±0.05	0.76±0.02
K_m (mM)	0.28±0.01	0.92±0.03	0.65±0.03	0.24±0.01
k_{cat}/K_m ($s^{-1}mM^{-1}$)	3.18±0.23	1.43±0.06	1.71±0.07	3.17±0.04